African Journal of Advanced Pure and Applied Sciences (AJAPAS)
Online ISSN: 2957-644X
Volume 2, Issue 3, July-September 2023, Page No: 296-308
Website: *https://aaasjournals.com/index.php/ajapas/index*
||Arab Impact factor 2022: 0.87|| SJIFactor 2023: 5.689|| ISI 2022-2023: 0.557

Anisotropy of Microstructure and Mechanical Properties in Low Carbon Steel Plates Additively Manufactured Using Gas Metal Arc Welding

Hassan Ali Saadawi[1*], Adel M. Daw[2], Hesham R. Eshabani[3], Mohamed A. Saraj[4]
[1,2,3,4] Advanced Occupational Center for Welding Technologies, Tripoli, Libya

[*]*Corresponding author: saadawi.hassan.74@gmail.com*

Received: July 13, 2023	Accepted: September 01, 2023	Published: September 04, 2023

Abstract:
In recent years, additive manufacturing (AM) for metals, which uses layer-by-layer deposition of materials to construct nearly net-shaped items, has attracted interest as a way to improve the effectiveness of production processes in a variety of industries. One of the latest developments in additive manufacturing techniques is Wire arc additive manufacturing (WAAM). In this work, a low carbon steel wall has been wire arc additively manufactured (WAAM) using the gas metal arc welding technique. an anisotropic behaviour of microstructure and mechanical properties such as impact toughness, yield strength, ultimate tensile strength, and the percentage of elongation have been investigated in three different directions, vertical (90°), horizontal (0°) and diagonal (45°). The pearlite fractions in Top, front and diagonal planes were 18.45%, 16.14% and 17.76% respectively. These variations of pearlite fraction affect the mechanical properties of the additively manufactured wall; the anisotropic percentages of ultimate tensile strength and impact toughness for the vertical and horizontal directions were 13.63 % and 9.42 % respectively, relatively higher than those of horizontal and diagonal directions.

Keywords: Wire Arc Additive Manufacturing (WAAM), Gas Metal Arc Welding, Anisotropy, Impact Toughness.

Cite this article as: H. A. Saadawi, A. M. Daw, H. R. Eshabani, M. A. Saraj, "Anisotropy of Microstructure and Mechanical Properties in Low Carbon Steel Plates Additively Manufactured Using Gas Metal Arc Welding: A Study of Rainfall Patterns," *African Journal of Advanced Pure and Applied Sciences (AJAPAS)*, vol. 2, no. 3, pp. 296–308, July-September 2023.

تباين البنية المجهرية والخواص الميكانيكية في ألواح الصلب منخفض الكربون المصنعة بالإضافة باستخدام لحام القوس المستهلك والغازات الخاملة والنشطة

حسن علي السعداوي[1*]، عادل محمد ضو[2]، هشام رمضان الشعباني[3]، محمد اعمار السراج[4]
[1،2،3،4] المركز الليبي المهني المتقدم لتقنيات اللحام، طرابلس، ليبيا

الملخص
في السنوات الأخيرة، اجتذب التصنيع الإضافي (AM) للمعادن، والمتمثل في تصنيع منتجات بترسيب المواد طبقة تلو الأخرى، الاهتمام كوسيلة لتحسين جودة عمليات الإنتاج في العديد من الصناعات. أحد أحدث التطورات في تقنيات التصنيع بالإضافة هو التصنيع الإضافي بالسلك والقوس (WAAM). في هذا العمل، تم تصنيع جدار من الصلب منخفض الكربون بطريقة التصنيع الإضافي بالسلك والقوس (WAAM) باستخدام لحام القوس المستهلك والغازات الخاملة والنشطة. تم دراسة تباين البنية المجهرية والخواص الميكانيكية مثل مقاومة الصدم، مقاومة الخضوع، مقاومة

الشد القصوى، ونسبة الاستطالة في ثلاث اتجاهات مختلفة، عمودي (90 درجة)، أفقي (0 درجة) وقطري (45 درجة). كانت نسبة البيرلايت في المستوى العلوي والأمامي والقطري 18.45%، 16.14% و17.76% على التوالي. هذه الاختلافات في نسبة البيرلايت تؤثر على الخواص الميكانيكية للجدران المصنعة بشكل إضافي، حيث كانت نسب التباين في قوة الشد القصوى ومقاومة الصدم للاتجاهين الرأسي والأفقي 13.63% و9.42% على التوالي، وهي أعلى نسبياً من تلك الخاصة بالاتجاهين الأفقي والقطري.

الكلمات المفتاحية: التصنيع الإضافي بالسلك والقوس (WAAM)، لحام القوس المستهلك والغازات الخاملة، تباين الخواص، مقاومة الصدم.

1. Introduction

Manufacturing companies face intense competition; therefore, they must constantly work on product development to get a competitive edge. Companies need also keep up with changes in manufacturing technologies, such as additive manufacturing. This is due to the symbiotic relationship between technology and product development; successful products can only be produced with the best lead-time if both are improved concurrently [1, 2].

Additive manufacturing (AM) refers to layer-by-layer and down-up manufacturing technology based on the deposition principle without using any additional resources such as cutting tools and cooling fluid [3,4,5,6].

The use of metal additive manufacturing (AM) has increased recently across a number of sectors, including the aerospace, military, automotive, oil, and medical industries. Powder Bed Fusion Additive Manufacturing (PBF) and Directed Energy Deposition Additive Manufacturing (DED) are the two basic categories into which metal AM processes can be divided. In PBF AM, a heat source fuses layers of material in powder form. The products are created in the DED AM by layering material in the form of wire or sheets and fusing it with heat [7,8].

Weld metal deposition to produce functional surfaces or structures is not a recent development. Build-up welding is a widely used technique for surfacing or repair purposes. The basic idea of using arc welding to produce precise shaped items was originally introduced in 1925. The technology, which is now commonly referred to as Wire + arc additive manufacturing (WAAM), has gained considerable interest because to recent advancements in additive manufacturing of metals and new arc technologies process [9].

Wire arc additive manufacturing process (WAAM) deposits a metal wire using an arc heat source. In the WAAM process, a traditional welding machine may be used as a heat source that decreases the initial investment costs compared to the laser and electron beam heat sources. In addition, the cost of raw materials of the wire type is roughly 10 per cent of the cost of raw materials of the powder type [6,10,11]. The WAAM process therefore produces a high deposition rate at a low cost, making it a highly favoured process for the manufacturing of large components using expensive materials [12,13,14].

The WAAM technique may be used with a variety of materials, such as steels, Inconel, and titanium, and it is frequently used with expensive materials to create close-to-net-shape items that minimize material waste [15]. Among different materials, Steel is the most used materials in many sectors of engineering. Therefore, steel is most studied materials for WAAM as well. the changes of microstructural and property during welding and additive manufacturing are widely understood but still under investigation [4,16]. Due to sequential melting and solidification in wire arc additive manufacturing process, each region of the part is subjected to different thermal cycles which lead to anisotropic behaviour of microstructure and mechanical properties. Therefore, it is important to investigate the anisotropic behaviour of WAAM'd parts [13,17,18,19].

Few studies have investigated the anisotropy of microstructure and mechanical properties of carbon steel additively manufactured parts. Rafieazad et al. [20] studied the tensile properties of the fabricated WAAM-ER70S-6 part and obtained comparable yield and ultimate tensile strengths along the building (vertical) direction and deposition (horizontal) direction. However, the ductility along the horizontal direction was approximately three times higher than that of the vertical direction. Same results have been reported by Ghaffari et al. [21] the tensile strength of the component was found to be isotropic, whereas the ductility of the fabricated samples revealed significant anisotropy. Also, no obvious anisotropy in mechanical properties have been observed by Haden et al. [22]. On the other hand, Le et al. [23] reported the anisotropic mechanical properties in WAAM low-carbon steel walls. Nagasai et al. [24] studied the impact toughness of cylindrical wall component in the vertical direction and compare the results with (ER70S-6 filler metal).

The following work is based on the deposition of successive layers to build up a wall of low carbon steel (ER70S-6) and will be carried out in two phases, the initial study aims to achieve the optimum process parameters. And, the second phase of the work will focus on anisotropic behaviour of microstructure and mechanical properties such as impact toughness, yield strength, ultimate tensile strength, and the percentage of elongation in three different directions such as building (vertical) (90°), deposition (horizontal) (0°) and diagonal (45°) directions.

2. Experimental Work

2.1 Materials

Two steels have been employed in this experimental work:

1- Low carbon steel plate St 37 with the dimensions of 500 mm × 200 mm × 10 mm were used as substrates to carry out the experiments. This work was focused only on the AM layers and did not include the interface layer.

2- Low carbon steel (ESAB OK Autrod 12.51) filler wire which was standardized as per SFA/AWS A5.18 : ER70S-6 and EN ISO 14341-A : G 38 2 C1 Z 3Si1 was used as the feedstock material in the experiments [25]. The chemical composition of ER70S-6 filler material and low carbon steel St 37 are shown in Table 1 [26].

Table 1. Chemical composition of ER70S-6 and St 37

Alloy /Wt.%	C	Mn	Si	P	S	Ni	Cr	Mo	Fe
ER70S-6	.07	1.25	0.76	0.015	0.0053	0.008	0.014	0.002	Bal.
St 37	0.15	0.491	0.073	0.008	0.009	0.03	0.001	0.008	Bal.

2.2 Wire Arc Additive Manufacturing Procedure

2.2.1 Equipment

The system used to perform additive manufacturing deposition is composed by the integration of two different systems:

- Welding system. In this work, the semi-automatic ESAB LKB 265 GMAW machine was used as the WAAM process. This WAAM method provides high deposition rate.
- Three-axis movement system, the motion of the system should be easily controlled.

The power source and movement system used for the described experimental work in this section is shown in the Figure 1-a.

2.2.2 Sample Build-up

Gas metal arc welding technique was used to deposit all beads. A reversed polarity (electrode positive) direct current (DCEP) between the wire electrode and the substrate was used in all runs. A wall with the size of 280 mm × 12 mm × 120 mm was deposited using ER70S-6 carbon steel filler metal. The substrate was St 37 carbon steel plate. The plate was cleaned to remove dirt, located at flat position, aligned on the platform and clamped manually. After clamping, the beads are built using back strep strategy (the same direction of deposition see Figure 1-b). When a deposit was completed, the torch back to the starting point of the next deposit, and an idle interpass time of 60 s was applied to cool down the walls by the atmosphere until 40 layers of material were deposited using mechanized torch. Schematic WAAM setup could be seen in Figure 1-c. The employed welding parameters were kept constant for all deposited layers as given in the Table 2. To protect the weld pool from atmospheric contamination a mixture of Ar + 2% O2 was used as shielding gas.

Table 2. Welding parameters

Parameter	Setting
Welding process	GMAW
Welding position	PA (1G)
Average current	185 A
Average voltage	28 V
Welding speed	250 mm/min
Wire feed rate	3.5 m/min
Wire diameter	1.2 mm
Shielding gas flow rate	18 L/min
Contact tube distance	10 mm

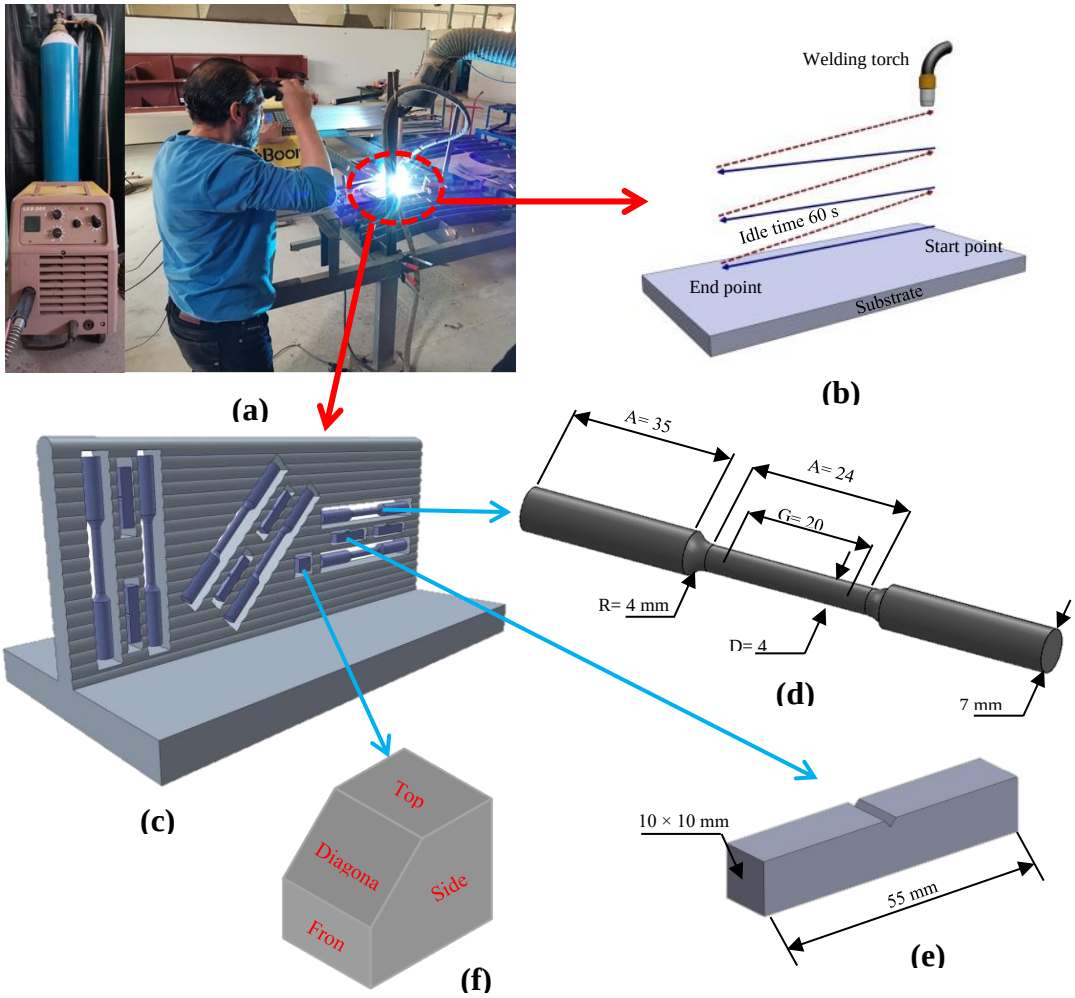

Figure 1. Schematic diagram of the WAAM process: (a) Process setup, (b) Deposition strategy, (c) WAAM'd wall with sampling position, (d) Tensile specimen, (e) Impact specimen, (f) Microstructural examination specimen.

2.3 Integrity Assessment of the Additively Manufactured Beads

2.3.1 Appearance and Macroscopic Characterization

Deposited beads performed by WAAM were visually inspected to check surface imperfections. Then dimensions of manufactured part, as shown in Figure 1-c, were measured. After visual inspection, a sample from transverse side of WAAM'd wall was taken for macroscopic examination. The sample was etched using (Ammonium Persulfate at room temperature)

2.3.2 Surface Waviness

One of the most crucial factors used to assess the WAAM deposition quality is surface waviness. Surface waviness was defined as the maximum crest-to-trough distance measured on cross section from the deposited wall as illustrated in Figure 2 [27, 28]. ImageJ 1.5j8 image processing software was used to measure the surface [29]. Five equally spaced (10 mm from each other) measurements of width and height were performed for deposited wall, waviness and material usage efficiency were computed according to Equation (1) and (2), and the average and standard deviation values were calculated [28].

$$Surface\ waviness\ (SW) = \frac{(Wm - We)}{2} \quad (1)$$

$$Material\ usage\ efficiency\ (MUE) = \left(\frac{We - 2SW}{We}\right) \times 100 \quad (2)$$

Where: Wm is maximum width and We is effective width

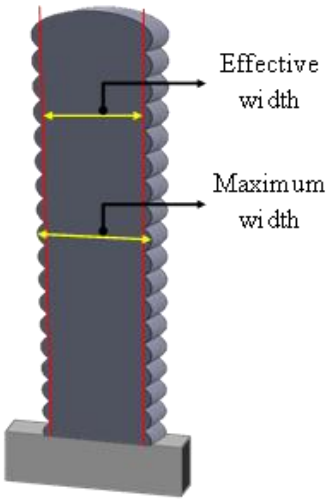

Figure 2. Surface waviness measurements.

2.4 Mechanical Characterization

2.4.1 Tensile Test

For observing tensile properties of built materials, six round tensile specimens were sectioned from the additively manufactured wall of ER70S-6 steel filler material, two parallel to building (vertical) (90°), two parallel to deposition (horizontal) (0°) and two parallel to diagonal (45°) directions as seen in Figure 1-c . Tensile samples were prepared according to ASTM E8 standard [30], Figure 1-d shows the dimensions of the samples. The tensile tests were conducted on HST universal testing machine model WDS-50E at room temperature.

2.4.2 Impact Test

Charpy impact tests have been performed on Six specimens having dimensions 10x10x55 mm at room temperature according to ASTM E23 standard [31], Figure 1-e shows the dimensions of the samples. The specimens were sectioned from WAAM'd wall and vee notched in three different directions, two parallel to building (vertical) (90°), two parallel to deposition (horizontal) (0°) and two parallel to diagonal (45°) directions as seen in figure 1-c. the impact test were executed using Zwick/ Roell test machine.

2.4.3 Hardness Test

The hardness of built materials was measured in three regions of cross section from the deposited wall: the upper, middle and lower region Figure 3. The hardness was measured at four locations in each region. The indentations were made under the load of 30 Kg over 15 s with a distance of 0.3 mm between the indentations according to IS0 6507.1 standard [32].

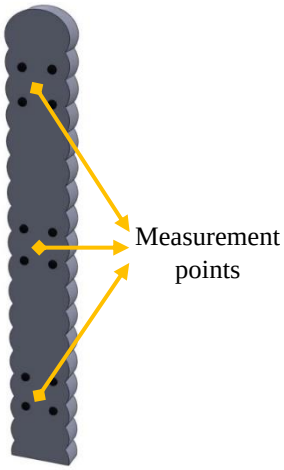

Figure 3. Hardness measurements

2.5 Microstructural Examination

To perform microstructural examination and investigate possible microstructural anisotropy in the WAAM'd wall, four samples from middle location of the wall, including the front, side, top, and the diagonal view were sectioned

(illustrated in Figure 1-f). Specimens were hot-mounted in conductive bakelite, grinded and polished using 9, 6 and 1 µm colloidal alumina suspension, then etched by 5% Nital for 20 s. The microstructure of all specimens was examined using HST Metallurgical Microscope Model: 402-AW.

3 Results and Discussion

3.1 Integrity Assessment of the Additively Manufactured Beads

3.1.1 Appearance and Macroscopic Characterization

Three-dimensional shape of the wire arc additively manufactured wall made by ER70S-6 low carbon steel filler metal is shown in Figure 4, displaying the geometrical measurements of the manufactured part.

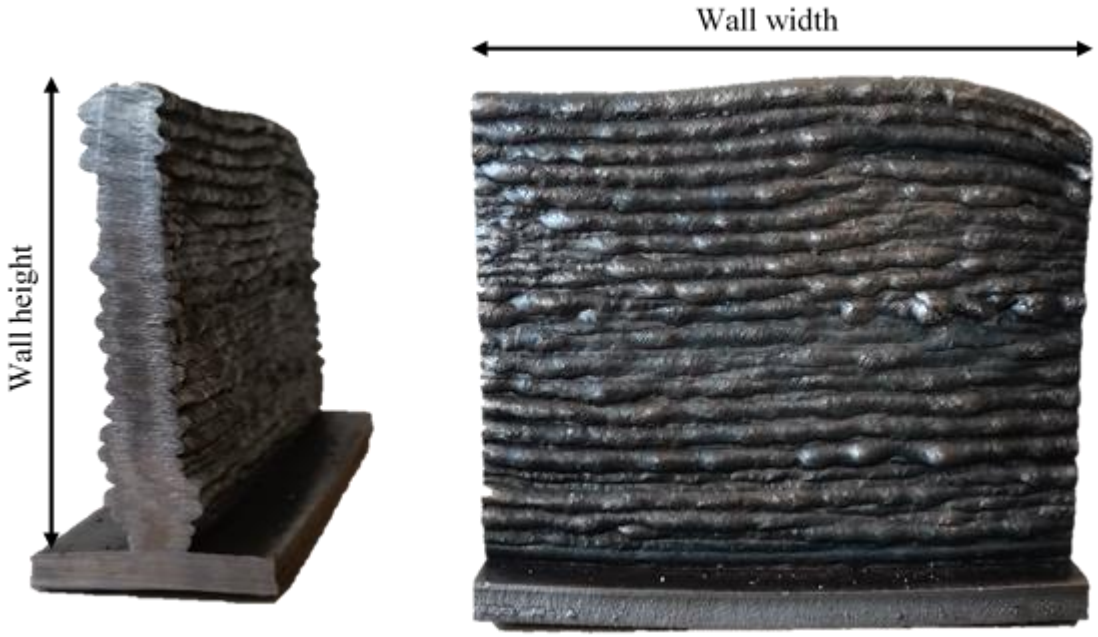

Figure 4. Geometrical measurements of the manufactured part

A sample from transverse side of WAAM'd wall, as shown in Figure 5-a, was cut for surface waviness measurements and macroscopic examination. The surface waviness of the built wall was measured using ImageJ 1.5j8 image processing software [29], as shown in Figure 5-b. Table 3 presents the average values of width, height, waviness and material usage efficiency.

Table 3. Geometrical measurements of the manufactured part

Measurements (mm)	Number of Measurements	Average (mm)
Wall width	5	11.964
Wall height	5	123.368
Thickness of the layer	5	2.462
Surface waviness	5	1.387
Material usage efficiency	5	69.82 %

The macro-image of the wall shows the built-up layers which bands in a concave shape (see Figure 5-b). The additively manufactured part was free of cracks and no lack of fusion or volumetric discontinuities were detected. These findings indicating the suitability of using GMAW as WAAM technique to construct a wall of low carbon steel with high density, strong layer bonds, and without major imperfections.

a b

Figure 5. Cross-section and macro-image of the wall**.**

3.2 Microstructure Characterization

Figure 6 shows the 3-D representation of the microstructural morphologies in the middle region of the as-deposited ER70S-6 low carbon steel wall produced using WAAM. Figure 6 showed the presence of pearlite in ferrite matrix. The white regions are ferrite and dark areas are pearlite. The middle region of wall reveals polygonal coarse granular structures of ferrite with low volume fraction of pearlite at grain boundaries.

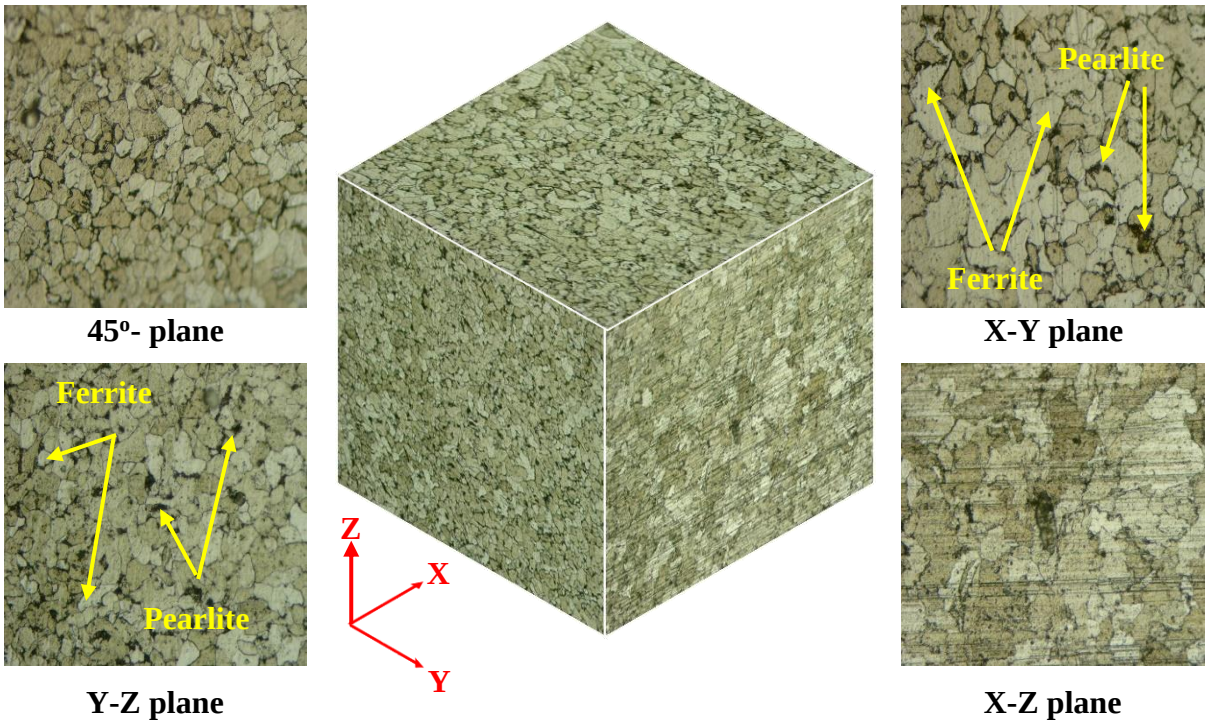

Figure 6. 3-D representation of the microstructural in the middle region of wall

This microstructure of low carbon steel with low amount of pearlite also obtained after an arc welding process, according to Jafarzadegan et al. [33]. The reduction of pearlite amount is due to the differences in carbon content

and inherent rapid solidification characteristics of the WAAM process [26]. Mechanically**,** the properties of pearlite are in between ductile ferrite and the hard cementite [34]. As result, the low pearlite content AM wall lead to reduction of in strength, hardness and ductility as compared to the reference ER70S-6 filler metal and ST-37 alloy.
On the other hand, the microstructure of the reference ER70S-6 low carbon steel filler metal presented a regular ferrite matrix and pearlite phase, as shown in Figure 7.

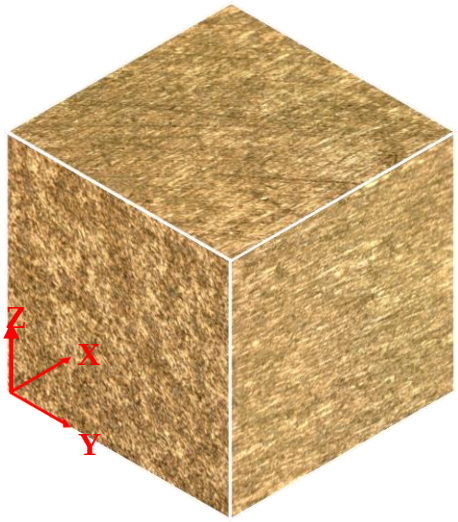

Figure 7. 3-D representation of the microstructural ER70S-6 low filler metal

The ferrite/pearlite ratio is an important microstructural parameter affecting the properties of steel. Unbalanced ferrite/ pearlite ratio influences the anisotropy behaviour of mechanical properties, and therefore, investigations are required. The ferrite/ pearlite ratio can be measured using a variety of techniques, including point counting (PC) and image analysis (IA). IA is a quick method but demands high quality microstructural images and computer software packages [36,37]. Top, front and diagonal microstructural images from additively manufactured wall , see figure 8, were chosen to determine the ferrite/ pearlite ratio using image analysis approach. The ferrite/ pearlite ratio was calculated using ImageJ 1.5j8 image analysis software [29].
As shown in Figure 8-a, the pearlite fraction in Top plane was 18.45%, whereas Figure 8-b shows that the pearlite percentage in the front plane was 16.14%. The pearlite percentage in diagonal plane is 17.76%. These microstructural changes, expectedly, changes the mechanical properties.

3.3 Mechanical Characterization

3.3.1 Hardness Test

Table 4 presents the values of hardness in three zones of cross-section area: upper, middle and lower zone. Four points in each zone, as shown in Figure 3, was measured. In the WAAM'd wall, the lower region shows the higher hardness value than the middle and upper regions. The hardness of the constructed materials is found to be comparable to that of wrought St 37 steel (approximately 168 HV), which has chemical composition similar to ER70S-6 steel [5].

Table 4. Hardness values in three zones

	Regions	Point 1	Point 2	Point 3	Point 4	Average
Hardness values HV	Upper	155	160	155	162	158
	Middle	171	165	171	174	170
	Lowe r	185	178	185	182	183
	ER70S-6	--	--	--	--	198
	St 37	--	--	--	--	168

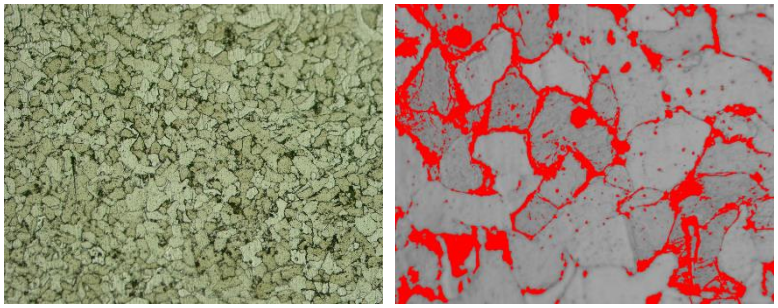

Measurement	Pearlite fraction
Area	18.45 %

(a)

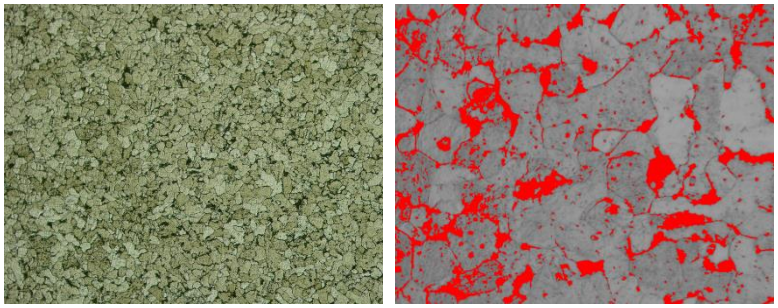

Measurement	Pearlite fraction
Area	16.14 %

(b)

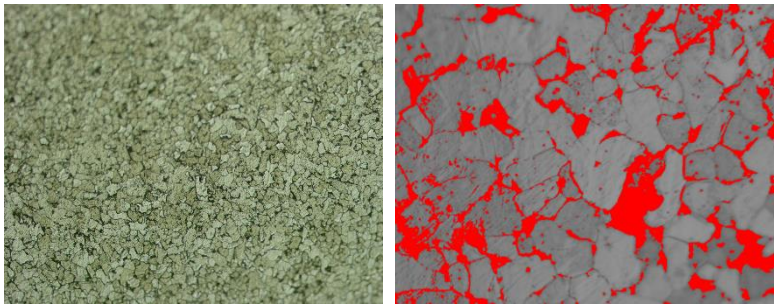

Measurement	Pearlite fraction
Area	17.76 %

(c)

Figure 8. Ferrite/pearlite ratio at the middle region of wall: (a) Top plane, (b) front plane , (c) diagonal plane

3.3.2 Tensile Test

As described in section 2.4.1 and illustrated in Figure 1-c, six tensile tests were conducted, two for each orientation. Figure 9 shows fractured samples after tension tests. Table 5 contains the tensile properties of examined samples and tensile properties from ER70S-6 steel data sheet [25].

Figure 9. Fractured samples after tension tests

Table 5. Mechanical properties of the manufactured part

SN	Yield strength (MPa)	Average (MPa)	Ultimate tensile strength (MPa)	Average (MPa)	elongation (%)	Average (%)
Vertical 1	398.09	330.414	565.61	501.75	23	20
Vertical 2	262.74		437.90		17	
Horizontal 1	406.05	414.011	566.96	570.14	20	25
Horizontal 2	421.97		573.33		30	
Diagonal 1	473.73	352.31	584.79	543.75	21	22
Diagonal 2	230.89		502.71		23	
ER70S-6		480		560		26

It can be found that the yield strength, ultimate tensile strength, and elongation values of vertical specimens are inferior to that of horizontal and diagonal specimens, confirming the anisotropic behaviour on these directions. The percentage of anisotropy is calculated by formula (3). [35]:

$$Ap = \frac{P_2 - P_1}{P_1} \qquad (3)$$

Where Ap is the anisotropic percentage, P1 and P2 represent the average value of properties of two directions respectively. The anisotropic percentages of yield strength, ultimate tensile strength, and elongation respectively come to:

- 25.30 %, 13.63 %, and 25 %, for the vertical and horizontal samples.
- 6.63 %, 8.37 %, and 10 %, for the vertical and diagonal samples.
- 17.51 %, 4.85 %, and 13.64 %, for the horizontal and diagonal samples.

3.3.3 Impact Test

Charpy tests have been performed in order to analyse the influence of the bead direction on the impact toughness. In the present study, Average values observed in the horizontal direction are similar to the ones observed in the diagonal direction and higher than the value in the vertical direction. Table 6 contains the impact toughness of examined samples, and Figure 10 shows fractured samples after impact tests.

Table 6. Impact toughness of the manufactured part

SN.	Impact toughness (J)	Average (J)
Vertical 1	153	138
Vertical 2	122	
Horizontal 1	150	151
Horizontal 2	153	
Diagonal 1	132	141
Diagonal 2	150	
ER70S-6	--	130

The anisotropic percentages of impact toughness come to:

- 9.42 %, for the vertical and horizontal samples.
- 2.17 %, for the vertical and diagonal samples.

- 7.09 %, for the horizontal and diagonal samples.

Figure 10. Fractured samples after impact tests

4. Conclusion

In this investigation, a low carbon steel wall was fabricated by wire arc additive manufacturing and an analysis on its mechanical properties and microstructure was done. The following conclusions can be drawn:

1. The GMAW-WAAM technique enables the construction of low carbon steel walls with high density and minimal defects such cracks and incorrect fusions between layers.
2. The microstructural of middle region of the as-deposited wall shows polygonal coarse granular structures of ferrite with low volume fraction of pearlite at grain boundaries, The pearlite fractions in Top, front and diagonal plane were 18.45%, 16.14% and 17.76% respectively.
3. The values of hardness in three zones of cross-section area: upper, middle and lower zone were 158, 170 and 185 respectively.
4. The anisotropic percentages of ultimate tensile strength and impact toughness for the vertical and horizontal directions were 13.63 % and 9.42 % respectively, relatively higher than those (4.85 % and 7.09 %) of horizontal and diagonal directions.

Acknowledgment

The authors acknowledge the funding and support from the Libyan Advanced Occupational Centre for Welding Technologies

References

[1] Staffanson, A., and P. Ragnartz. "Improving the product development process with additive manufacturing." PhD diss., MS thesis, Mech Eng., Mälardalens Univ., Västerås, Sweden, 2018.

[2] Köhler, Markus, Sierk Fiebig, Jonas Hensel, and Klaus Dilger. "Wire and arc additive manufacturing of aluminum components." *Metals* 9, no. 5 (2019): 608.

[3] Youheng, Fu, Wang Guilan, Zhang Haiou, and Liang Liye. "Optimization of surface appearance for wire and arc additive manufacturing of Bainite steel." *The International Journal of Advanced Manufacturing Technology* 91 (2017): 301-313.

[4] Sun, Laibo, Fengchun Jiang, Ruisheng Huang, Ding Yuan, Chunhuan Guo, and Jiandong Wang. "Microstructure and mechanical properties of low-carbon high-strength steel fabricated by wire and arc additive manufacturing." *Metals* 10, no. 2 (2020): 216.

[5] Van Thao, L. E. "A preliminary study on gas metal arc welding-based additive manufacturing of metal parts." *VNUHCM Journal of Science and Technology Development* 23, no. 1 (2020): 422-429.

[6] Zhang, Wenjie, Weining Lei, Yang Zhang, and Xiao Liu. "Microstructure and mechanical properties of wire arc additive-manufacturing high-carbon chromium bearing steel." *Mater. Technol* 54 (2020): 359-364.

[7] Rodrigues, Tiago A., Valdemar Duarte, Julian A. Avila, Telmo G. Santos, R. M. Miranda, and J. P. Oliveira. "Wire and arc additive manufacturing of HSLA steel: Effect of thermal cycles on microstructure and mechanical properties." *Additive Manufacturing* 27 (2019): 440-450.

[8] Kok, Yihong, Xi Peng Tan, Pan Wang, M. L. S. Nai, Ngiap Hiang Loh, Erjia Liu, and Shu Beng Tor. "Anisotropy and heterogeneity of microstructure and mechanical properties in metal additive manufacturing: A critical review." *Materials & Design* 139 (2018): 565-586.

[9] Plangger, Josef, Peter Schabhüttl, Tomaž Vuherer, and Norbert Enzinger. "CMT additive manufacturing of a high strength steel alloy for application in crane construction." *Metals* 9, no. 6 (2019): 650.

[10] Lee, Seung Hwan. "Optimization of cold metal transfer-based wire arc additive manufacturing processes using gaussian process regression." *Metals* 10, no. 4 (2020): 461.
[11] Cunningham, C. R., J. M. Flynn, Alborz Shokrani, Vimal Dhokia, and S. T. Newman. "Invited review article: Strategies and processes for high quality wire arc additive manufacturing." *Additive Manufacturing* 22 (2018): 672-686.
[12] Wächter, Michael, Marcel Leicher, Moritz Hupka, Chris Leistner, Lukas Masendorf, Kai Treutler, Swenja Kamper, Alfons Esderts, Volker Wesling, and Stefan Hartmann. "Monotonic and fatigue properties of steel material manufactured by wire arc additive manufacturing." *Applied Sciences* 10, no. 15 (2020): 5238.
[13] Ermakova, Anna, Ali Mehmanparast, Supriyo Ganguly, Nima Razavi, and Filippo Berto. "Fatigue crack growth behaviour of wire and arc additively manufactured ER70S-6 low carbon steel components." *International Journal of Fracture* 235, no. 1 (2022): 47-59.
[14] Laghi, Vittoria, Michele Palermo, Giada Gasparini, Valentina Alena Girelli, and Tomaso Trombetti. "Geometrical characterization of wire-and-arc additive manufactured steel element." *Advanced Materials Letters* 10, no. 10 (2019): 695-699.
[15] Weflen, E. D., M. A. Black, M. C. Frank, and F. E. Peters. "Wire Arc Additive Manufacturing of Low Carbon Steel for Casting Applications." In *2021 International Solid Freeform Fabrication Symposium*. University of Texas at Austin, 2021.
[16] Treutler, Kai, and Volker Wesling. "The current state of research of wire arc additive manufacturing (WAAM): a review." *Applied Sciences* 11, no. 18 (2021): 8619.
[17] Vahedi Nemani, Alireza, Mahya Ghaffari, and Ali Nasiri. "On the post-printing heat treatment of a wire arc additively manufactured ER70S part." *Materials* 13, no. 12 (2020): 2795.
[18] Shassere, Benjamin, Andrzej Nycz, Mark W. Noakes, Christopher Masuo, and Niyanth Sridharan. "Correlation of microstructure and mechanical properties of metal big area additive manufacturing." *Applied Sciences* 9, no. 4 (2019): 787.
[19] Sridharan, Niyanth, Mark W. Noakes, Andrzej Nycz, Lonnie J. Love, Ryan R. Dehoff, and Sudarsanam S. Babu. "On the toughness scatter in low alloy C-Mn steel samples fabricated using wire arc additive manufacturing." *Materials Science and Engineering: A* 713 (2018): 18-27.
[20] Rafieazad, Mehran, Mahya Ghaffari, Alireza Vahedi Nemani, and Ali Nasiri. "Microstructural evolution and mechanical properties of a low-carbon low-alloy steel produced by wire arc additive manufacturing." *The International Journal of Advanced Manufacturing Technology* 105 (2019): 2121-2134.
[21] Ghaffari, Mahya, Alireza Vahedi Nemani, Mehran Rafieazad, and Ali Nasiri. "Effect of solidification defects and HAZ softening on the anisotropic mechanical properties of a wire arc additive-manufactured low-carbon low-alloy steel part." *Jom* 71 (2019): 4215-4224.
[22] Haden, C. V., G. Zeng, F. M. Carter III, C. Ruhl, B. A. Krick, and D. G. Harlow. "Wire and arc additive manufactured steel: Tensile and wear properties." *Additive Manufacturing* 16 (2017): 115-123.
[23] Le, Van Thao, Tien Long Banh, Duc Toan Nguyen, and Van Tao Le. "Wire arc additive manufacturing of thin-wall low-carbon steel parts: Microstructure and mechanical properties." *International Journal of Modern Physics B* 34, no. 22n24 (2020): 2040154.
[24] Nagasai, Bellamkonda Prasanna, Sudersanan Malarvizhi, and Visvalingam Balasubramanian. "Mechanical properties of wire arc additive manufactured carbon steel cylindrical component made by gas metal arc welding process." *Journal of the Mechanical Behavior of Materials* 30, no. 1 (2021): 188-198.
[25] ESAB Team, "Welding Filler Metal Data book," ESAB, USA, 2016.
[26] Ron, Tomer, Galit Katarivas Levy, Ohad Dolev, Avi Leon, Amnon Shirizly, and Eli Aghion. "Environmental behavior of low carbon steel produced by a wire arc additive manufacturing process." *Metals* 9, no. 8 (2019): 888.
[27] Kazanas, Panagiotis, Preetam Deherkar, Pedro Almeida, Helen Lockett, and Stewart Williams. "Fabrication of geometrical features using wire and arc additive manufacture." *Proceedings of the Institution of Mechanical Engineers, Part B: Journal of Engineering Manufacture* 226, no. 6 (2012): 1042-1051.
[28] Geng, Haibin, Jinglong Li, Jiangtao Xiong, Xin Lin, Dan Huang, and Fusheng Zhang. "Formation and improvement of surface waviness for additive manufacturing 5A06 aluminium alloy component with GTAW system." *Rapid Prototyping Journal* 24, no. 2 (2018): 342-350.
[29] W. Rasband, ImageJ, National Institutes of Health, Bethesda, Maryland, USA, 1997-2018.
[30] ASTM Subcommitte E28.04, ASTM E8, "Standard Test Methods for Tension Testing of Metallic Materials," American Society for Testing and Materials, USA, 2013.
[31] ASTM Subcommitte E28.07, ASTM E23, "Standard Test Methods for Notched Bar Impact Testing of Metallic Materials," American Society for Testing and Materials, USA, 2002.

[32] The International Organization for Standardization, “Metallic materials – Vickers hardness test - Part 1: Test method,” ISO 6507-1, 2018.
[33] Jafarzadegan, M., A. H. Feng, A. Abdollah-Zadeh, T. Saeid, J. Shen, and H. Assadi. "Microstructural characterization in dissimilar friction stir welding between 304 stainless steel and st37 steel." *Materials Characterization* 74 (2012): 28-41.
[34] Grong, OaDKM, and David K. Matlock. "Microstructural development in mild and low-alloy steel weld metals." *International metals reviews* 31, no. 1 (1986): 27-48.
[35] Sun, Laibo, Fengchun Jiang, Ruisheng Huang, Ding Yuan, Chunhuan Guo, and Jiandong Wang. "Anisotropic mechanical properties and deformation behavior of low-carbon high-strength steel component fabricated by wire and arc additive manufacturing." *Materials Science and Engineering: A* 787 (2020): 139514.
[36] ASTM Subcommitte E04.14, ASTM E562, “Standard Test Method for Determining Volume Fraction by Systematic Manual Point Count,” American Society for Testing and Materials, USA, 2011.
[37] ASTM Subcommitte E04.14, ASTM E1245, “Practice for Determining the Inclusion or Second Phase Constituent Content of Metals by Automatic Image Analysis,” American Society fot Testing and Materials, USA, 2011.